Fano effect in the angle-integrated valence band photoemission of the noble metals Cu, Ag, and Au

C. De Nadaï,[1] J. Minár,[2] H. Ebert,[2] G. Ghiringhelli,[3] A. Tagliaferri,[3] and N. B. Brookes[1]
[1]*European Synchrotron Radiation Facility, Boîte Postale 220, 38043 Grenoble Cedex, France*
[2]*Department Chemie, Phys. Chemie, Universität München, Butenandtstr. 5-13, D-81377 München, Germany*
[3]*INFM-Dip. di Fisica, Politecnico di Milano, p. Leonardo da Vinci 32, 20133 Milano, Italy*
(Received 20 February 2004; revised manuscript received 23 June 2004; published 15 October 2004)

Results of a combined experimental and theoretical investigation on the Fano-effect in the angle-integrated valence band photoemission of the noble metals are presented. In line with the fact that the Fano-effect is caused by the spin-orbit-coupling, the observed spin polarization of the photocurrent was found to be the more pronounced the higher the atomic number of the element investigated. The ratio of the normalized spin difference curves, however, agreed only for Cu and Ag with the ratio of the corresponding spin-orbit coupling strength parameters. The deviation from this expected behavior in the case of Au could be explained by the properties of individual *d-p*- and *d-f*-contributions to the total spin difference curves, that were found to be quite different for Au compared to Cu and Ag.

DOI: 10.1103/PhysRevB.70.134409 PACS number(s): 82.80.Pv, 71.15.Rf, 71.20.Be, 71.70.Ej

I. INTRODUCTION

The term Fano-effect denotes the observation that one may obtain a spin-polarized photocurrent even for a nonmagnetic sample if one is using polarized light within a photoemission experiment. Originally, the effect was discussed by Fano for free atoms exposed to circularly polarized light.[1,2] In particular, he could demonstrate that the spin polarization of the photoelectrons to be observed is a direct consequence of spin-orbit coupling and the selection rules imposed by the polarization of the light. The Fano-effect could first be demonstrated experimentally by Heinzmann *et al.* for free Cs atoms[3] and also for Cs films.[4] Subsequent work could demonstrate the Fano-effect for many different systems in angle-integrated as well as angle-resolved photoemission.[5] In particular, for semiconductors a very pronounced spin polarization of the photocurrent can be achieved by tuning the frequency of the exciting light to the band-gap energy. In the case of GaAs a spin-polarization of 50% can in principle be achieved[6] supplying this way a very simple and efficient laboratory source for spin-polarized electron beams.

The pioneering work of Fano was later on followed by various theoretical studies for solids.[7,8] In particular, a detailed fully relativistic description of angle-resolved photoemission was developed by several authors[9–12] on the basis of the so-called one-step model of photoemission. From corresponding investigations Feder and co-workers concluded that the Fano-effect should not be restricted to experiments using circularly polarized radiation but should also be present if linearly polarized radiation is used in combination with a low symmetry surface of the sample.[13] This prediction could indeed be verified by a subsequent experiment.[14] These theoretical investigations as well as the present one, used an itinerant description of the underlying electronic structure. In contrast to this Thole and van der Laan adopted an atomic point of view to deal with spin-resolved photoemission experiments.[15] On this basis these authors derived sum rules that connect the spin-difference of the photoemission spectra with ground state properties.

Recently, Ghiringhelli *et al.*[16] investigated experimentally the Fano-effect in angle-integrated valence band x-ray photoemission spectroscopy (VB-XPS). A corresponding fully relativistic description of this experiment was presented by Minar *et al.*[17] that allowed a detailed discussion of the experimental results for Cu. Experiment and calculations have also been compared for Ag.[18] Accompanying analytical studies and model calculations have shown in particular that the Fano-effect in angle-integrated VB-XPS is a first-order effect with respect to spin-orbit coupling. From this interrelation a corresponding increase of the observed spin-polarization is expected along the sequence Cu-Ag-Au.[19] The new experimental and theoretical results to be presented essentially confirm this expectation. However, they also demonstrate that the relative weight of the *d-p* and *d-f* excitation channels may have a strong impact on the observed spin polarization. In the next section a short description of our experimental and theoretical approach is given. This is followed by the presentation of results for Cu, Ag, and Au together with a detailed discussion.

II. EXPERIMENT

The experiments were performed at the European Synchrotron Radiation Facility (ESRF) at Grenoble. The copper spectra was previously measured on ID12B at the ESRF (Refs. 16 and 17) and the silver and gold samples were measured on the high flux ID08 beamline. This beamline is equipped with a APPLEII helical undulator providing ~100% circularly polarized soft x rays (10^{13} photons/s/0.1% BW) in addition to vertical and horizontally linear polarization. The photon energy range of the beamline is from 400 to 1500 eV. The silver spectra reproduced, with much better statistics the spectra reported before[18] and the gold spectra have never been reported before. The spin-resolved photoemission spectra were measured using a 140 mm mean radius hemispherical analyzer coupled to a mini-Mott 25 kV spin polarimeter with an effi-

ciency (Sherman function Seff) of 17%.[20] The samples were high purity polycrystalline metallic foil scrapped *in situ* to remove surface contamination and the cleanliness was checked using core-level photoemission (XPS). The pressure in the spectrometer was $<10^{-10}$ mbar. The combined energy resolution was ≈ 0.6 eV and each spectra took several hours to measure. All measurements were made at room temperature. The angular acceptance of the analyzer was +20°. Together with the polycrystalline nature of the samples this means that the measurement is angle integrated. The angle between the photon beam and the analyzer was 60°. The measurements were carried out at normal emission. Since the propagation direction of the photons defines the spin direction, there is a 30° angle between the direction of the spins and the spin analyzer. The spin polarized measurements are corrected for this geometrical factor and the Sherman function. The spin-resolved spectra were recorded for the two spin directions (measured simultaneously) and for both $\pm$ light helicities in order to eliminate the systematic errors introduced by the experimental apparatus.

III. THEORETICAL FRAMEWORK

The theoretical results to be presented below have been obtained by applying the one-step model of photoemission.[21,22] A corresponding fully relativistic description of spin-resolved and angle-integrated valence-band photoemission has been derived by Ebert and Schwittalla[23] that led to the following expression for the photocurrent:

$$I(E,m_s;\omega,\mathbf{q},\lambda) \propto \Im \sum_{\Lambda\Lambda''} C_{\Lambda}^{-m_s} C_{\Lambda''}^{-m_s} \Bigg\{ \sum_{\Lambda_1\Lambda_2} \tau^{00}_{\Lambda_1\Lambda_2}(E) \times \Bigg[\sum_{\Lambda'} t^{0}_{\Lambda'\Lambda}(E') M^{\vec{q}\lambda}_{\Lambda'\Lambda_1} \Bigg] \times \Bigg[\sum_{\Lambda'''} t^{0}_{\Lambda'''\Lambda''}(E') M^{\vec{q}\lambda}_{\Lambda'''\Lambda_2} \Bigg]^{*} - \sum_{\Lambda'\Lambda'''\Lambda_1} t^{0}_{\Lambda'\Lambda}(E') I^{\vec{q}\lambda}_{\Lambda'\Lambda_1\Lambda'''} t^{0*}_{\Lambda'''\Lambda''}(E') \Bigg\}. \quad (1)$$

Here, excitation of valence band electrons at energy E by radiation with frequency ω, wave vector $\mathbf{q}$ and polarization λ has been considered. For the final state at energy $E'=E+\hbar\omega$ multiple scattering events are ignored (single scatterer approximation)[24,25] because of the high photon energies used in the experiments to be discussed below. For the same reason the influence of the surface can be neglected implying that the photocurrent given by Eq. (1) is determined by the scaling properties of the bulk regime. Using fully relativistic multiple scattering theory[26] to represent the underlying electronic structure, the single-site t-matrices $t_{\Lambda\Lambda'}$ and the scattering path operator $\tau^{00}_{\Lambda\Lambda'}$ occurring in Eq. (1) are used in the so-called Λ-representation with $\Lambda=(\kappa,\mu)$ standing for the relativistic spin-orbit coupling and magnetic quantum numbers, κ and μ, respectively. Finally, the matrix elements $M^{\vec{q}\lambda}_{\Lambda\Lambda'}$ and $I^{\vec{q}\lambda}_{\Lambda\Lambda'\Lambda''}$ are the dipole matrix elements connected with the regular and irregular initial state wave functions, Z_{Λ} and J_{Λ}, respectively. (For further details, see Ref. 23.)

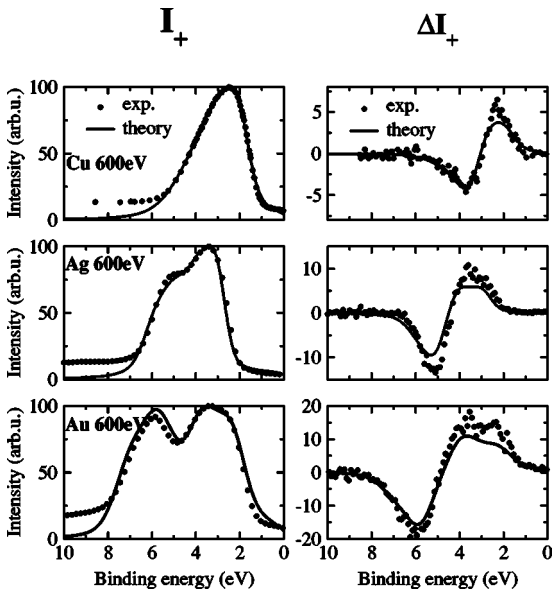

FIG. 1. (Left) Spin and angle-integrated VB-XPS emission intensity I of Cu, Ag, and Au for a photon energy of 600 eV. (Right) Spin-difference $\Delta I_{+}=I_{+}^{\uparrow}-I_{+}^{\downarrow}$ of the photocurrent for excitation with circularly polarized radiation. Theory: full line; experiment: dots.

For the polar geometry used in the experiments with the spin polarization $\Delta I_{\lambda}=I_{\lambda}^{\uparrow}-I_{\lambda}^{\downarrow}$ measured with respect to the direction of the incoming photon beam, ΔI_{Λ} can be obtained directly by applying Eq. (1) for the spin quantization axis chosen along the photon beam. For more complex geometries an appropriate extension of Eq. (1) according to spin matrix formalism can be used.[27]

To allow for a direct comparison of the theoretical spectra with experiment one has to account for various intrinsic and experimental broadening mechanisms. For the spectra presented below, the influence of finite lifetimes have been represented by a Lorentzian broadening using an energy dependent width $\Gamma(E)=a+b(E-E_F)^2$ with E_F the Fermi energy (Cu: $a=0.1$ eV, $b=0.01$ eV^{-2}; Ag: $a=0.01$ eV, $b=0.02$ eV^{-2}; Au: $a=0.001$ eV, $b=0.001$ eV^{-2}) and an energy independent one corresponding to the kinetic energy of the final state ($\Gamma=0.1$ eV, as calculated from the universal curve of electron attenuation length). In addition, a Gaussian broadening has been applied (Cu: $\Gamma=0.4$ eV; Ag: $\Gamma=0.4$ eV; Au: $\Gamma=0.4$ eV).

IV. RESULTS AND DISCUSSION

The experimental VB-XPS intensities I and spin differences $\Delta I_{\lambda}=I_{\lambda}^{\uparrow}-I_{\lambda}^{\downarrow}$ obtained for a photo energy of 600 eV for Cu, Ag, and Au, that have been normalized to have a maximum amplitude of 100, are summarized in Fig. 1 (The Cu-spectra have been reproduced from Ref. 17). The corresponding theoretical spectra, that have been broadened as described above, reproduce the experimental data obviously quite well. For the photocurrent intensity I deviations of the

theoretical spectra from the experimental ones occur primarily for higher binding energies. Presumably, these deviations have to be ascribed first of all to the contributions of secondary electrons, that have to be subtracted from the experimental total photocurrent to deduce the primary photocurrent intensity.

The photocurrent spectra shown in Fig. 1 are by far dominated by initial states having *d*-character. For that reason, they primarily reflect the main features of the *d*-band complexes of the noble metals. While for Cu the spectrum show only some asymmetry, a shoulder on the low energy side clearly shows up for Ag. This trend is continued by Au, for which a clear splitting of the spectrum with two main peaks is observed (see below). These changes are accompanied by an increase of the *d*-band width from about 2 eV for Cu to 4 and 6 eV for Ag and Au, respectively. This increase of the *d*-band width is primarily caused by the fact that the number of nodes of the radial wave function increases when going from a 3*d*- to a 4*d*- and finally to a 5*d*-element. As a consequence of the increasing number of nodes, the *d*-states get less localized leading to a larger band width. For Au the spin-orbit coupling contributes in addition to the band width in quite an appreciable way. This can be seen from the energy splitting ΔE_{SOC} of the resonances of the $d_{3/2}$- and $d_{5/2}$-phase shifts, that represents the strength of the spin-orbit coupling in an average way ignoring its dependency on energy and wave vector that might be present for Bloch-type band states $\psi_{n\mathbf{k}}(E)$. The spin-orbit coupling parameter ΔE_{SOC} defined this way increases rapidly with increasing atomic number (Cu: 0.27 eV; Ag: 0.52 eV; and Au: 1.41 eV) taking an appreciable value for Au and leading to a corresponding contribution to the *d*-band width. An additional consequence of this is that the peak at 6 eV binding energy stems primarily from electrons having $d_{3/2}$-character, while for the peak at 3 eV binding energy electrons with $d_{5/2}$-character dominate.

As was shown in detail in Ref. 17 the spin-polarization observed in the angle-integrated photocurrent obtained from nonmagnetic samples and excitation with circularly polarized light is due to the presence of the spin-orbit coupling. In particular from the analytical model considerations presented in Ref. 17 together with values for the average spin-orbit coupling parameter ΔE_{SOC} given above, one expects that the amplitudes of the normalized spin difference ΔI_{λ} should increase by a factor of 2 or 5 when going from Cu to Ag or Au, respectively. Figure 1 indeed confirms that the maximum spin difference of Ag is indeed twice that of Cu. However, comparing the spin differences of Cu and Au one finds only an increase by a factor of 3 instead of 5. This discrepancy could be caused by higher order corrections with respect to the spin-orbit coupling that might be important for Au. More important, however, seems to be the relative contribution of the *d-p*- and *d-f*-excitation channels for the resulting spin difference. As it was shown analytically and numerically in Ref. 17 both contributions differ in sign for a given helicity of the radiation. In addition, their dependency on the photon energy may be quite different. For Cu the *d-f*-excitation is larger by about one order of magnitude than the *d-p*-absorption for photon energies higher than about 50 eV. For decreasing photon energies the *d-p*-absorption grows more rapidly than the *d-f*-excitation leading to a more or less vanishing spin difference at about 20 eV followed by a change in sign of the spin difference spectrum for a further decrease in the photon energy. For a photon energy of 600 eV, used to record the spectra shown in Fig. 1, the *d-p*- and *d-f*-partial spin differences of Cu have nearly the same spectral shape but reversed sign (see Fig. 2 in Ref. 17 and the similar spin difference curves of Au shown below in Fig. 4. This also holds for the spin difference spectra of Ag. In particular it turns out that for 600 eV photon energy the calculated ratio of the *d-f*- to the *d-p*-contribution to the spin difference is nearly the same for Cu and Ag; namely −16.1:1 for Cu and −17.1:1 for Ag, respectively. This finding explains why the increase of the spin difference exactly follows the increase of the spin-orbit coupling strength when going from Cu to Ag. On the other hand these considerations clearly show that the change of the spin difference with the atomic number will not follow the change of ΔE_{SOC} if the relative weight of the *d-p*- and *d-f*-excitation channels change. This exactly happens for Au, for which the result −3.5: 1 have been obtained from our calculations for the ratio of the *d-f*- and *d-p*-contributions to the spin difference at a photon energy of 600 eV. This means that in contrast to Cu and Ag the *d-f*-spin difference of Au is compensated in an appreciable way by the *d-p*-spin difference leading to an increase of the spin difference when going from Cu to Au that is much smaller than expected on the basis of the spin-orbit splittings parameter ΔE_{SOC} alone.

In fact it turns out that the spin difference ΔI_{λ} of Au depends much more on the photon energy as found before for Cu (see Fig. 2). This is because of the larger weight of the *d-p*-channel in the case of Au, and the strong variation of the *d-p*- and *d-f*-excitation with photon energy. As Fig. 3 shows there is a pronounced Cooper minimum for the *d-f* channel at around 220 eV photon energy.[28,29] In addition one finds a less pronounced minimum at 480 eV with corresponding maxima at about 350 and 650 eV. The position of the minima correlate quite well with the centers of the 7*f*- and 9*f*-canonical bands of Au, that are derived from the logarithmic derivative of the radial wave functions.[30] In the same way, the maxima can be connected with the 8*f*- and 10*f*-bands. This close correlation reflects the fact that the sequence of minima and maxima is caused by the increase of the number of nodes in the radial wave function when the energy of the final state increases. The variation of the *d-p*-absorption with photon energy shown in Fig. 3 leads to a dominance of this channel for photon energies between about 150 and 280 eV. In addition it contributes in an appreciable way at around 500 eV because of the coincidence of a maximum in the *d-p*-absorption and a minimum in the *d-f*-excitation channel. A corresponding sequence of spin difference spectra resolved according to the absorption channel is shown in Fig. 4, that obviously reflects the dependence of the photocurrent intensity on the photon energy. In particular it can be seen from this figure that the *d-p*-contribution dominates around the Cooper minimum of the *d-f*-channel and has a rather appreciable weight for all other photon energies as well. As a consequence our calculations predict a pronounced decrease of the total spin difference of Au when changing the photon energy from

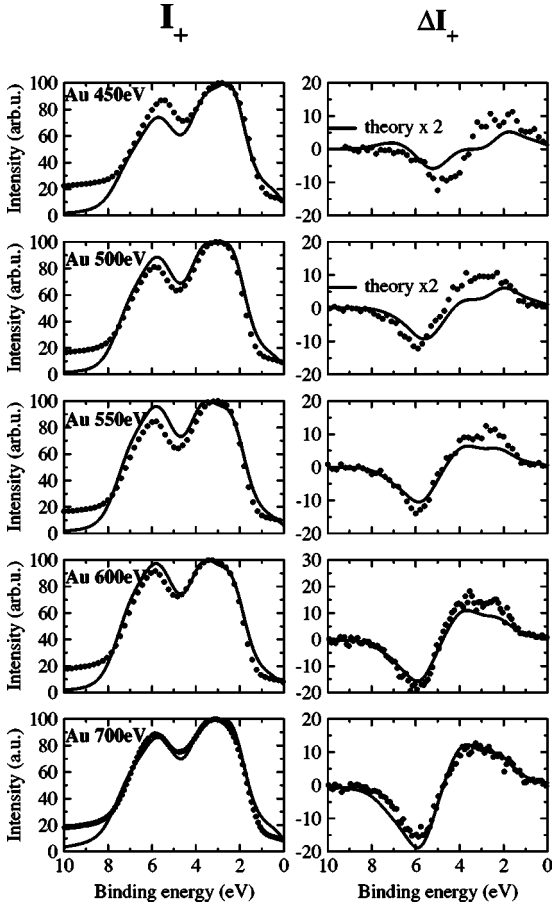

FIG. 2. (Left) Spin and angle-integrated VB-XPS emission intensity I of Au for different photon energies. (Right) Spin-difference $\Delta I_+ = I_+^{\uparrow} - I_+^{\downarrow}$ of the photocurrent for excitation with circularly polarized radiation. Theory: full line; experiment: dots.

600 to 500 eV and an increase upon a change to 700 eV. As one can see in Fig. 2 the experimental spectra indeed follow these expectations, while the changes are not as pronounced as found for the theoretical spectra. On the theoretical site, this deviation could be ascribed to some extent to the use of the single-scatterer approximation for the final states. Another source could be the use of the atomic sphere approxi-

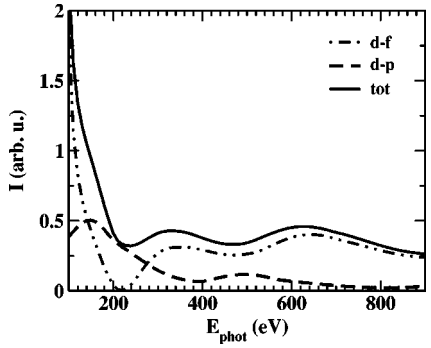

FIG. 3. Decomposition of the theoretical photoemission intensity I of Au into its dominating d-p- and d-f-contributions as a function of the photon energy. The energy of the initial state has been fixed to −2 eV with respect to the Fermi energy.

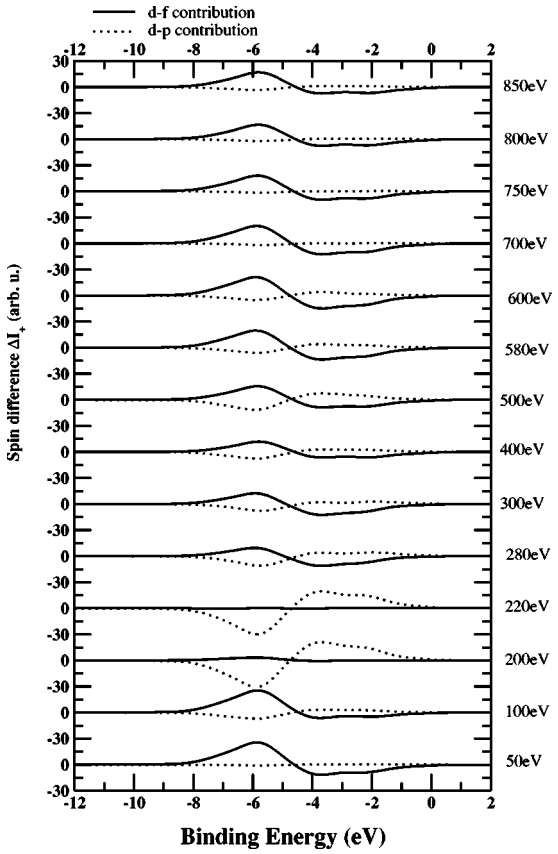

FIG. 4. Decomposition of the theoretical spin-difference of the photo current $\Delta I_+ = I_+^{\uparrow} - I_+^{\downarrow}$ of Au according to the angular momentum character of the initial and final states for various photon energies. Only the dominating d-p (dotted line) and d-f (full line) contributions are shown.

mation (ASA) that could have an influence on the relative weight of the d-p- and d-f-matrix elements. Nevertheless, in accordance with the calculations the experimental spin difference ΔI_λ shown in Fig. 1 changes its spectral shape within about −5 and −1 eV in a pronounced way. This change is connected with the relative weight of the d-p- and d-f-contributions to ΔI_λ and their individual spectral shape. Comparing the various ΔI_λ-curves for Au in Fig. 4 with the corresponding ones of Cu (see Fig. 2 in Ref. 17) one notes that for the d-f-curves there is a minimum at −3.5 eV and at −5.7 eV for Cu and Au, respectively. For Cu a maximum occurs at −2 eV while there is a double peak structure in the case of Au with maxima at −3.7 and −2 eV. A very similar situation is present for the d-p-part or the ΔI_λ curves that have a different sign and their main spectral features slightly shifted. As a consequence of these properties the spectral shape of the spin difference ΔI_λ of Au changes between −5 and −1 eV in an appreciable way if the photon energy is varied. As Fig. 1 shows the peak in the ΔI_λ-curve at −3.8 eV is more pronounced than at −2 eV for a photon energy of 700 eV. Decreasing the photon energy to 600 eV leads to peak heights that are essentially the same. This trend is continued for 500 eV photon energy for which the peak at −2 eV is more pronounced.

Thole and van der Laan[15] derived sum rules which shows that the spin-difference and the integrated intensity are pro-

portional to the ground state expectation values of the spin-orbit coupling. In spite of the very appealing feature of the sum rules of Thole and van der Laan[15] to connect spin-resolved photoemission spectra to the ground state expectation values of spin and orbital momentum products, one has to keep in mind that in deriving these rules a number of assumptions had to be made. The main restriction is that only one angular momentum character of the final states had been assumed corresponding to $\Delta l = +1$ transitions. In the case of Cu and Ag this restriction is justified according to our numerical results. On the other hand because of the important contribution of the *d*-*p* transitions to the spin difference in the Fano effect of Au the $l = -1$ transitions need to be taken into account when applying the sum rules.

V. SUMMARY

A combined experimental and theoretical investigation of the Fano-effect in the spin-integrated VB-XPS of Cu, Ag, and Au has been presented. In line with the origin of the Fano-effect, namely the presence of the spin-orbit coupling, an increase of the normalized spin-difference is found with increasing atomic number. While the ratio of the spin-differences of Cu and Ag strictly follow the ratio of the spin-orbit coupling strength the data for Au seem to be in conflict with this relationship. The reason for this behavior could be traced back to the change in the relative weight of the *d*-*p*- and *d*-*f*-channel. In particular it could be shown that the *d*-*p*-channel is much more important for Au than for Cu and Ag and that the ratio of the *d*-*p* and *d*-*f*-contributions change in a pronounced way in the case of Au.

ACKNOWLEDGMENT

This work was funded by the German BMBF (Bundesministerium für Bildung und Forschung) under Contract No. 05 KS1WMB/1.

[1] U. Fano, Phys. Rev. **184**, 250 (1969).
[2] U. Fano, Phys. Rev. **178**, 131 (1969).
[3] U. Heinzmann, J. Kessler, and J. Lorenz, Z. Phys. **240**, 42 (1970).
[4] U. Heinzmann, K. Jost, J. Kessler, and B. Ohnemus, Z. Phys. **251**, 354 (1972).
[5] U. Heinzmann and G. Schönhense, *Polarized Electrons in Surface Physics*, edited by R. Feder (World Scientific, Singapore, 1985), p. 467.
[6] D. T. Pierce and F. Meier, Phys. Rev. B **13**, 5484 (1976).
[7] K. Koyama and H. Merz, Z. Phys. B **20**, 131 (1975).
[8] G. Borstel and M. Wöhlecke, Phys. Rev. B **26**, 1148 (1982).
[9] B. Ackermann and R. Feder, J. Phys. C **18**, 1093 (1985).
[10] B. Ackermann and R. Feder, Solid State Commun. **54**, 1077 (1985).
[11] B. Ginatempo, P. J. Durham, B. L. Gyorffy, and W. M. Temmerman, Phys. Rev. Lett. **54**, 1581 (1985).
[12] J. Braun, Rep. Prog. Phys. **59**, 1267 (1996).
[13] E. Tamura, W. Piepke, and R. Feder, Phys. Rev. Lett. **59**, 934 (1987).
[14] B. Schmiedeskamp, B. Vogt, and U. Heinzmann, Phys. Rev. Lett. **60**, 651 (1988).
[15] B. T. Thole and G. van der Laan, Phys. Rev. Lett. **70**, 3479 (1993).
[16] G. Ghiringhelli, H. Tjeng, A. Tanaka, O. Tjernberg, T. Mizokawa, J. L. de Boer, and N. B. Brookes, Phys. Rev. B **66**, 075101 (2002).
[17] J. Minár, H. Ebert, G. Ghiringhelli, O. Tjernberg, N. B. Brookes, and L. H. Tjeng, Phys. Rev. B **63**, 144421 (2001).
[18] J. Minár, H. Ebert, L. H. Tjeng, P. Steeneken, G. Ghiringhelli, O. Tjernberg, and N. B. Brookes, Appl. Phys. A: Mater. Sci. Process. **73**, 663 (2001).
[19] A. R. Mackintosh and O. K. Andersen, *Electrons at the Fermi Surface* (Cambridge University Press, Cambridge, 1980), Chapter on the Electronic Structure of Transition Metals.
[20] G. Ghiringhelli, K. Larsson, and N. B. Brookes, Rev. Sci. Instrum. **70**, 4225 (1999).
[21] P. J. Feibelman and D. E. Eastman, Phys. Rev. B **10**, 4932 (1974).
[22] R. Feder, *Polarized Electrons in Surface Physics* (World Scientific, Singapore, 1985), p. 125.
[23] H. Ebert and J. Schwitalla, Phys. Rev. B **55**, 3100 (1997).
[24] T. Jarlborg and P. O. Nilson, J. Phys. C **12**, 265 (1979).
[25] H. Winter, P. J. Durham, and G. M. Stocks, J. Phys. F: Met. Phys. **14**, 1047 (1984).
[26] H. Ebert, in *Electronic Structure and Physical Properties of Solids*, Vol. 535 in Lecture Notes in Physics, edited by H. Dreyssé (Springer, Berlin, 2000), p. 191.
[27] J. Minár, Ph.D. thesis, Logos Verlag Berlin, University of Munich, 2003.
[28] G. Rossi, I. Lindau, L. Braicovich, and I. Abbati, Phys. Rev. B **28**, 3031 (1983).
[29] S. L. Molodtsov, S. V. Halilov, V. D. P. Servedio, W. Schneider, S. Danzenbächer, J. J. Hinarejos, M. Richter, and C. Laubschat, Phys. Rev. Lett. **85**, 4184 (2000).
[30] H. L. Skriver, *The LMTO-Method* (Springer, Berlin, 1983).